

This is the accepted manuscript made available via CHORUS, the article has been published as:

Possible multigap superconductivity and magnetism in  
single crystals of superconducting  $\text{La}_{\{2\}}\text{Pt}_{\{3\}}\text{Ge}_{\{5\}}$   
and  $\text{Pr}_{\{2\}}\text{Pt}_{\{3\}}\text{Ge}_{\{5\}}$

N. H. Sung, C. J. Roh, K. S. Kim, and B. K. Cho

Phys. Rev. B **86**, 224507 — Published 14 December 2012

DOI: [10.1103/PhysRevB.86.224507](https://doi.org/10.1103/PhysRevB.86.224507)

# Possible multi-gap superconductivity and magnetism in single crystals of superconducting $\text{La}_2\text{Pt}_3\text{Ge}_5$ and $\text{Pr}_2\text{Pt}_3\text{Ge}_5$

N. H. Sung<sup>1</sup>, C. J. Roh<sup>2</sup>, K. S. Kim<sup>3</sup> and B. K. Cho<sup>1,2,a</sup>

<sup>1</sup>*School of Materials Science and Engineering,*

*Gwangju Institute of Science and Technology (GIST), Gwangju 500-712,*

*Korea* <sup>2</sup>*Department of Photonics and Applied Physics,*

*Gwangju Institute of Science and Technology (GIST),*

*Gwangju 500-712, Korea* <sup>3</sup>*Semiconductor Laboratory,*

*Samsung Advanced Institute of Technology (SAIT), Yongin 446-712, Korea*

## Abstract

We herein describe our investigation of the superconducting and magnetic properties of the rare-earth ternary germanide intermetallic compounds  $\text{La}_2\text{Pt}_3\text{Ge}_5$  and  $\text{Pr}_2\text{Pt}_3\text{Ge}_5$ . Single crystals of  $\text{La}_2\text{Pt}_3\text{Ge}_5$  and  $\text{Pr}_2\text{Pt}_3\text{Ge}_5$  were synthesized using the high temperature metal flux method. Both types of crystal formed in a  $\text{U}_2\text{Co}_3\text{Si}_5$ -type orthorhombic structure (space group  $Ibam$ ).  $\text{La}_2\text{Pt}_3\text{Ge}_5$  showed the onset of superconducting phase transition at  $T_c = 8.1$  K, which, to the best of our knowledge, is the highest  $T_c$  of all the  $RE_2TM_3X_5$  ( $RE$  = Rare Earth elements,  $TM$  = Transition metal, and  $X = s - p$  metal) superconductors, and from the specific heat data, it was found to have multi-gap superconductivity.  $\text{Pr}_2\text{Pt}_3\text{Ge}_5$  showed both a superconducting phase transition at  $T_c = 7.8$  K and two antiferromagnetic transitions at  $T_{N1} = 3.5$  K and  $T_{N2} = 4.2$  K, which indicates the coexistence of superconductivity and magnetism. However, the correlation between the superconductivity and the magnetism was too weak to be observed. In its normal state,  $\text{Pr}_2\text{Pt}_3\text{Ge}_5$  revealed strong magnetic anisotropy, probably due to the crystalline electric field effect.

<sup>a</sup> Corresponding author : chobk@gist.ac.kr

## I. INTRODUCTION

$RE_2TM_3X_5$  ( $RE$  = Rare Earth elements,  $TM$  = Transition metal, and  $X = s-p$  metal, also known as '235 compounds') have been investigated for decades, because of their interesting magnetic[1–15] and superconducting properties.[8–17] Most magnetic 235 compounds exhibit a number of interesting properties, such as antiferromagnetic (AF) ordering,[2–15] metamagnetic phase transition (MMT),[5, 6] high magnetoresistance (MR),[6, 10] the crystalline electric field effect (CEF),[4–12] Kondo lattice,[1–4, 10–12] and heavy Fermion (HF) behavior.[5, 10, 14] These interesting characteristics lend these compounds to studies of various novel ground states by the substitution of different elements in them. For example,  $Ce_2Rh_3Ge_5$  shows AF ordering with HF behavior, and  $Pr_2Rh_3Ge_5$  shows HF behavior without any phase transition, while  $Pr_2Pd_3Ge_5$  only shows AF ordering and MMT.[5, 6, 10] Moreover, superconductivity occurs when pressure is applied to  $Ce_2Ni_3Ge_5$ , which has AF ordering, and re-entrant superconducting behavior is observed in  $Tm_2Fe_3Si_5$ , where AF ordering affects the superconductivity.[13, 14] Among the superconducting 235 compounds,  $Lu_2Fe_3Si_5$  has been the focus of particularly intensive research because of its relatively high superconducting phase transition temperature of  $T_c \sim 6$  K and its two-gap superconducting structure.[17] More recently, fully opened superconducting gaps were confirmed by measuring specific heat,[18] penetration depth,[19] and thermal conductivity.[20] Furthermore, different anisotropies of the two bands in  $Lu_2Fe_3Si_5$  was also recently reported.[21] Because of their various interesting properties, the search for new 235 compounds that might possess higher  $T_c$  with magnetic ordering is of great importance to the study of superconductivity, magnetism and the relationship between them.

In the compound  $RE_2Fe_3Si_5$ , Fe atoms have no magnetic moment, but rather build large densities of states at the Fermi level,[13] we were therefore motivated to induce a larger density of the  $d$ -state by substituting Pt in the Fe sites. In the present study, we report the discovery of superconductivity (possibly with multi-gap) in  $La_2Pt_3Ge_5$ , which has the highest transition temperature ( $T_c = 8.1$  K) of all the 235 compounds, and we also show that  $Pr_2Pt_3Ge_5$  has both superconductivity at  $T_c = 7.8$  K and AF orderings at  $T_{N1} = 3.5$  K and  $T_{N2} = 4.2$  K, which indicates the coexistence of superconductivity and magnetism.

## II. EXPERIMENTAL DETAILS

Single crystals of  $\text{La}_2\text{Pt}_3\text{Ge}_5$  and  $\text{Pr}_2\text{Pt}_3\text{Ge}_5$  were grown by the high temperature flux method using a Pt-Ge mixture as a self-flux. Pieces of La (99.9%)(or Pr(99.9%)), Pt (99.99%), and Ge (99.999%) were placed in an alumina crucible in an atomic ratio of La (or Pr) : Pt : Ge = 1 : 4 : 20. The crucibles were sealed in quartz tubes under a pressure of 1/3 atm of Ar gas and placed vertically in a programmable box furnace. The furnace was heated at a rate of 200 °C/h to 1130 °C, maintained at 1130 °C for 40 hours, and then cooled to 850 °C at a rate of 3 °C/h. As a result, we obtained shiny single crystals of  $\text{La}_2\text{Pt}_3\text{Ge}_5$  and  $\text{Pr}_2\text{Pt}_3\text{Ge}_5$  (the insets of Fig. 1) after separating the grown crystals from the flux using a centrifuge with quartz wool as a filter. The characterization of crystals was performed using powder x-ray diffraction (XRD; Rigaku, RINT2000), field-emission scanning electron microscopy (SEM; Hitachi S-4700), and energy-dispersive x-ray (EDX; Horiba 7200-H) spectroscopy. XRD was performed at room temperature and the unit cell parameters were refined using PowderCell software; the alignment of the samples was confirmed using XRD techniques. Temperature- and field-dependent magnetizations of single crystals were measured using a superconducting quantum interference device magnetometer (SQUID; Quantum Design MPMS XL). Electrical resistivity was measured using a four-probe method with a LR700 resistance bridge, combined with a SQUID temperature control system. Heat capacity was measured using a Quantum Design physical property measurement system (PPMS), together with the relaxation technique.

## III. RESULTS AND DISCUSSION

Several crystals were pulverized in order to obtain powder XRD results for  $\text{La}_2\text{Pt}_3\text{Ge}_5$  and  $\text{Pr}_2\text{Pt}_3\text{Ge}_5$  [Fig. 1]. The structure of the compounds were formed in  $\text{U}_2\text{Co}_3\text{Si}_5$ -type orthorhombic structure (space group  $Ibam$ ). By refining the powder XRD data, the lattice parameters were determined to be  $a = 10.1508(5)$  Å,  $b = 12.0300(2)$  Å, and  $c = 6.2709(2)$  Å for  $\text{La}_2\text{Pt}_3\text{Ge}_5$ , and  $a = 10.1333(5)$  Å,  $b = 11.8600(1)$  Å, and  $c = 6.2288(6)$  Å for  $\text{Pr}_2\text{Pt}_3\text{Ge}_5$ , as shown in Fig. 1(a) and (b). The insets of Fig. 1 show the morphological shape of the single crystals of  $\text{La}_2\text{Pt}_3\text{Ge}_5$  and  $\text{Pr}_2\text{Pt}_3\text{Ge}_5$ . SEM images showed large flat surfaces with minor impurities on the surface of each sample (not shown here), and a quantitative



analysis of the EDX spectra was used to estimate the composition of  $\text{La}_{2.1}\text{Pt}_{2.8}\text{Ge}_{5.1}$  and  $\text{Pr}_{2.1}\text{Pt}_{2.9}\text{Ge}_{5.0}$ , which were close to the ideal chemical compositions of the crystals within an acceptable margin of error.

The temperature-dependent magnetization of  $\text{La}_2\text{Pt}_3\text{Ge}_5$  and  $\text{Pr}_2\text{Pt}_3\text{Ge}_5$  single crystals was measured and plotted in Fig. 2. Measurement of magnetization were performed with  $H = 10$  Oe with zero-field cooling (ZFC) and field-cooling warmup (FCW) processes with the field parallel and perpendicular to the  $a$ -axis for  $\text{La}_2\text{Pt}_3\text{Ge}_5$  and to the  $c$ -axis for  $\text{Pr}_2\text{Pt}_3\text{Ge}_5$ ; see Figs. 2(a) and (b), respectively. Bulk superconductivity was confirmed in both compounds and the superconducting transition temperatures were found to be  $T_c = 8.1$  K for  $\text{La}_2\text{Pt}_3\text{Ge}_5$  and  $T_c = 7.8$  K for  $\text{Pr}_2\text{Pt}_3\text{Ge}_5$ . Interestingly, these values of  $T_c$  are very similar to those of other  $RE\text{-Pt-Ge}$  ternary compounds,  $\text{LaPt}_4\text{Ge}_{12}$  ( $T_c = 8.3$  K) and  $\text{PrPt}_4\text{Ge}_{12}$  ( $T_c = 7.9$  K).[22] It may be seen that both  $\text{La}_2\text{Pt}_3\text{Ge}_5$  and  $\text{Pr}_2\text{Pt}_3\text{Ge}_5$  are typical type-II superconductors with low  $H_{c1}$  values, and that relatively large magnetic anisotropy was observed in  $\text{Pr}_2\text{Pt}_3\text{Ge}_5$ , while no anisotropy was seen in  $\text{La}_2\text{Pt}_3\text{Ge}_5$ , as shown in the insets of Figs. 2(a) and (b). Isothermal magnetization was measured as a function of the magnetic field at  $T = 2$  K for single crystals of  $\text{La}_2\text{Pt}_3\text{Ge}_5$  and  $\text{Pr}_2\text{Pt}_3\text{Ge}_5$ , as shown in Figs. 3(a) and (b), respectively. In the  $ab$  plane of  $\text{Pr}_2\text{Pt}_3\text{Ge}_5$ , there are magnetic phase transitions around  $H = 18$  kOe and  $H = 24$  kOe [Fig. 3(b)], and the Meissner effect and vortex pinning may be seen in the low field region [the inset of Fig. 3(b)]. We also observed magnetic hysteresis around  $H = 18$  kOe, which implies a first order phase transition. The saturated magnetic moment at  $H = 5$  T ( $M_s \approx 1 \mu_B$ ) is smaller than the theoretical Hund's rule ground state,  $g\mu_B J$  for an isolated  $\text{Pr}^{3+}$  ion ( $3.58 \mu_B/\text{Pr}^{3+}$ ), which is similar to the isostructural compounds,  $\text{Pr}_2\text{Pd}_3\text{Ge}_5$  and  $\text{Pr}_2\text{Ni}_3\text{Ge}_5$ . [5, 6] We believe that such a large magnetic anisotropy as well as low  $M_s$  value ( $\approx 1 \mu_B$ ) is probably due to the CEF effect.

Figure 4(a) shows the dc magnetization divided by the magnetic field, in the low temperature region, and Fig. 4(b) shows the inverse dc magnetization divided by the magnetic field, in terms of temperature at  $H = 1$  kOe with the field parallel ( $H\parallel c$ ) and perpendicular ( $H\parallel ab$ ) to the  $c$ -axis for  $\text{Pr}_2\text{Pt}_3\text{Ge}_5$ . In Fig. 4(a), the magnetization in the  $ab$  plane was found to be larger than that along the  $c$ -axis. For  $H\parallel ab$ , magnetic phase transitions were observed at  $T_{N1} = 3.5$  K and  $T_{N2} = 4.2$  K, while the diamagnetic superconducting signal was observed near  $T_{N1} = 3.5$  K for  $H\parallel c$ . By measuring the ZFC and FCW processes in the  $ab$  plane at  $H = 1$  kOe, we were able to observe magnetic hysteresis because of the Meissner

effect. It is therefore likely that magnetic ordering and superconductivity coexist with magnetic anisotropy in single crystals of  $\text{Pr}_2\text{Pt}_3\text{Ge}_5$ . The quite similar magnetic characteristics of anisotropy and two magnetic transitions was also observed in  $\text{Pr}_2\text{Pd}_3\text{Ge}_5$ , indicating that the two compounds of  $\text{Pr}_2\text{Pt}_3\text{Ge}_5$  and  $\text{Pr}_2\text{Pd}_3\text{Ge}_5$  have the almost same magnetic structure, although the former is superconducting and the latter is not.[5] In Fig. 4(b), the magnetizations for both directions follow the temperature dependence of the Curie Weiss law at high temperatures ( $150 \text{ K} \leq T \leq 300 \text{ K}$ ). By fitting the data to the Curie Weiss law, the effective magnetic moment was estimated to be  $\mu_{\text{eff}}(H\|c) = 3.69 \mu_{\text{B}}/\text{Pr}$  and  $\mu_{\text{eff}}(H\|ab) = 3.65 \mu_{\text{B}}/\text{Pr}$  for the field parallel and perpendicular to the  $c$ -axis, respectively. The values are comparable to the  $\mu_{\text{eff}}$  values for an isolated  $\text{Pr}^{3+}$  ion. The Weiss temperatures were also estimated to be  $\theta(H\|c) = -40.35 \text{ K}$  and  $\theta(H\|ab) = -54.63 \text{ K}$ . The large difference between  $\theta(H\|c)$  and  $\theta(H\|ab)$ , and the anisotropy below  $T \leq 150 \text{ K}$ , as shown in Fig. 3(b), are believed to be due to the CEF effect, where the environmental charges around  $\text{Pr}^{3+}$  ions produce a local electric field.

Figure 5 shows the temperature-dependent electrical resistivity in a zero field, with a current parallel to the  $ab$  plane for  $\text{La}_2\text{Pt}_3\text{Ge}_5$  and to the  $c$ -axis for  $\text{Pr}_2\text{Pt}_3\text{Ge}_5$ . The resistivity in the normal state exhibits metallic behavior in the temperature range  $9 \text{ K} \leq T \leq 300 \text{ K}$  for both compounds. The inset of Fig. 5 is an expanded plot in the low temperature region, which shows the superconducting phase transitions at  $T_c = 8.1 \text{ K}$  and  $T_c = 7.8 \text{ K}$  for single crystals of  $\text{La}_2\text{Pt}_3\text{Ge}_5$  and  $\text{Pr}_2\text{Pt}_3\text{Ge}_5$ , respectively, which is consistent with the transition temperatures obtained from the  $M - T$  data. For  $\text{Pr}_2\text{Pt}_3\text{Ge}_5$ , the resistivity below the superconducting transition shows no discernable change, i.e., re-entrance behavior, at  $T = T_{N1}$  or  $T_{N2}$ . We therefore envisage that the magnetic fluctuation near the AF ordering does not disturb the superconductivity in this compound, probably due to the weak interaction between the superconductivity and the magnetism. In addition, the weak interaction is likely to make the superconducting state coexist with a large localized magnetic moments of  $\text{Pr}^{3+}$  ions.

Specific heat data ( $C_p$ ) were obtained for samples with masses of 32.0 mg for  $\text{La}_2\text{Pt}_3\text{Ge}_5$  and 14.7 mg for  $\text{Pr}_2\text{Pt}_3\text{Ge}_5$ . The results are shown in Fig. 6(a), in which sharp peaks may be seen at  $T_{N1} = 3.4 \text{ K}$  and  $T_{N2} = 4.1 \text{ K}$  for  $\text{Pr}_2\text{Pt}_3\text{Ge}_5$ , which correspond to the magnetic transition temperatures from the  $M - T$  curve in Fig. 4(a). However, we observed no noticeable superconducting jump either around  $T_c = 8.1 \text{ K}$  in  $\text{La}_2\text{Pt}_3\text{Ge}_5$ , or around

7.8 K in  $\text{Pr}_2\text{Pt}_3\text{Ge}_5$ . In order to verify the superconducting jump at  $T = T_c$ , we obtained the temperature-dependent  $C_p(T)$  in the normal state under a magnetic field of  $H = 2$  T, which is higher than  $H_{c2}$  at  $T = 2$  K, and subtracted them from the  $C_p$  data in the superconducting state without magnetic field. Figure 6(b) shows the electronic specific heat coefficient of  $\text{La}_2\text{Pt}_3\text{Ge}_5$  at zero magnetic field, i.e.,  $C_{el}/T$  divided by  $\gamma_n$ , plotted in terms of  $T/T_c$ . The specific heat jump at zero field ( $\Delta C$ ) relative to the normal state specific heat ( $C_n$ ),  $\Delta C/\gamma_n T_c$  at  $T_c$  is 0.36, which is much smaller than the value of 1.43 obtained from BCS theory.

In the inset of Fig. 6(b), we show a conventional Debye fit to the normal state data in the temperature range  $2 \text{ K} \leq T \leq 10 \text{ K}$  using  $C_p = C_{el} + C_{ph} = \gamma_n T + \beta T^3 + \delta T^5$ , with the normal state specific heat coefficient  $\gamma_n$  and the coefficients of the phononic contribution  $\beta$  and  $\delta$ . The parameters obtained are  $\gamma_n = 4.65 \text{ mJ/mol K}^2$ ,  $\beta = 1.18 \text{ mJ/mol K}^4$ , and  $\delta = 1.03 \times 10^{-2} \text{ mJ/mol K}^6$ . The large  $T^5$  term observed in the normal state specific heat indicates a complex phonon density of states, which is similar to the case of single crystals of  $\text{Lu}_2\text{Fe}_3\text{Si}_5$  [17, 18] and supports the possibility of multi-gap superconductivity.

The reduced jump in heat capacity data is similar to that of  $\text{Lu}_2\text{Fe}_3\text{Si}_5$ , which was verified to have two-gap superconductivity.  $\Delta C/\gamma_n T_c$ . In addition, the almost linear temperature dependence of  $C_{el}/T$  below  $T_c$  does not represent the behavior of a conventional BCS-type single gap but is rather an indication of a superconducting multi-gap. These two characteristics are also similar to the compound  $\text{LiFeAs}$ , which has a two-gap structure.[23, 24] We also found that the superconducting phase transition temperature of  $T_c = 7.7 \text{ K}$  in the measurement of  $C_p$  was lower than the magnetic and electrical value of  $T_c = 8.1 \text{ K}$ . This characteristic of different values of  $T_c$  obtained using magnetic and thermodynamic measurement was also reported for  $\text{LiFeAs}$ . [24] It is therefore seems likely that both compounds  $\text{La}_2\text{Pt}_3\text{Ge}_5$  and  $\text{Pr}_2\text{Pt}_3\text{Ge}_5$  have multi-gap superconductivity.

There are other possible origins for the the reduced normalized jump at  $T_c$  and the linear term below  $T_c$ , such as impurity and inhomogeneity. However, we could not observe any noticeable impurities in EDX measurement but the good crystallization of the samples by single crystal XRD measurement. Moreover, bulk superconductivity was confirmed from magnetization measurement (Fig. 2), i.e. over 70 % of the volume fraction with  $H = 10 \text{ Oe}$  for  $\text{La}_2\text{Pt}_3\text{Ge}_5$  single crystal along the  $a$ -axis and  $\text{Pr}_2\text{Pt}_3\text{Ge}_5$  single crystal along the  $c$ -axis, respectively. Even if we assume that there is a 30 % of inhomogeneous phases which is not

superconducting, the jump in the heat capacity measurement at  $T_c$  is much smaller than expected value. It would be of great interest to measure specific heat at low temperatures in order to understand the symmetry of the superconducting gap in more detail.

The magnetic moment of Pr as extracted from the Curie-Weiss law, Fig. 4(b), suggests nearly free Pr ions, which is in marked contrast with the moment seen at low temperatures, e.g. the magnetization would seem to saturate at a value close to  $1 \mu_B$ , Fig. 3(b), considerably smaller than the free magnetic moment of Pr. This suggests Kondo screening of the magnetic moments, and therefore the development of a Kondo lattice, in other words that this compound should behave as a heavy Fermion compound. But this is at odds with the very small  $\gamma_n$  coefficient extracted from heat capacity measurements, Fig. 6. The obvious conclusion is that the small moment is likely due to the particular crystalline electric field scheme of this compound. Therefore, the Pr moment behave as nearly localized moments even in the low temperature limit where superconductivity emerges. Superconducting state might coexist with such a large local moment likely due to weak interaction between superconducting pairs and local magnetic moments. The coexistence of superconductivity and magnetism can be found in many magnetic superconducting compounds. For example,  $\text{ErNi}_2\text{B}_2\text{C}$ , which is one of the well-known borocarbide superconductors, has superconducting transition at  $T_c = 10.5$  K and antiferromagnetic ordering temperature at  $T_N = 5.85$  K, where Er has larger value of free magnetic moment than Pr.[25]

#### IV. SUMMARY

Single crystals of the ternary germanide superconductors  $\text{La}_2\text{Pt}_3\text{Ge}_5$  and  $\text{Pr}_2\text{Pt}_3\text{Ge}_5$  were successfully fabricated using a metal self-flux method. Magnetization, electrical resistivity, and heat capacity were measured with the field along specific crystallographic directions.  $\text{La}_2\text{Pt}_3\text{Ge}_5$  exhibited the onset of a superconducting phase transition at  $T_c = 8.1$  K, which is the highest  $T_c$  of all the 235-type superconductors. Measurement of specific heat showed that there was substantial evidence of multi-gap superconductivity, such as the small value ( $= 0.36$ ) of  $\Delta C/\gamma_n T_c$ , the linear decrease of superconducting electronic specific heat, and a complex phonon density of states.  $\text{Pr}_2\text{Pt}_3\text{Ge}_5$  shows the coexistence of superconductivity ( $T_c = 7.8$  K) and an antiferromagnetically ordered state ( $T_{N1} = 3.5$  K and  $T_{N2} = 4.2$  K), and no observable correlation between superconductivity and magnetism.

## **Acknowledgments**

We would like to thank Y. M. Jang for the assistance in the heat capacity measurement. This study was supported by the Ministry of Education, Science and Technology of the Republic of Korea (2011-0028736), and the National Research Foundation of Korea (NRF) (Grant No. R15-2008-006-01002-0).

- 
- [1] Yogesh Singh and S. Ramakrishnan, Phys. Rev. B **68**, 054419 (2003)
  - [2] Yogesh Singh, S. Ramakrishnan, Z. Hossain, and C. Geibel, Phys. Rev. B **66**, 014415 (2002)
  - [3] Z. Hossain, S. Hamashima, K. Umeo, T. Takabatake, and C. Geibel, and F. Steglich, Phys. Rev. B **62**, 8950 (2000)
  - [4] N. S. Sangeetha, A. Thamizhavel, C. V. Tomy, Saurabh Basu, S. Ramakrishnan, and D. Pal, Phys. Rev. B **84**, 064430 (2011)
  - [5] V. K. Anand, Z. Hossain, and C. Geibel, Phys. Rev. B **77**, 184407 (2008)
  - [6] V.K. Anand, A.K. Nandy, S.K. Dhar, C. Geibel, Z. Hossain, J. Magn. Magn. Mater. **313**, 164 (2007)
  - [7] B. Becker, S. Ramakrishnan, D. Groten, S. Süllow, C.C. Mattheus, G.J. Nieuwenhuys, and J.A. Mydosh, Physica B **230-232**, 253 (1997)
  - [8] S. Ramakrishnan, N. G. Patil, Aravind D. Chinchure, and V. R. Marathe, Phys. Rev. B **64**, 064514 (2001)
  - [9] Yogesh Singh, D. Pal, and S. Ramakrishnan, Phys. Rev. B **70**, 064403 (2004)
  - [10] Z. Hossain, H. Ohmoto, K. Umeo, F. Iga, T. Suzuki, T. Takabatake, N. Takamoto and K. Kindo, Phys. Rev. B **60**, 10383 (1999)
  - [11] N. G. Patil and S. Ramakrishnan, Phys. Rev. B **59**, 12054 (1999)
  - [12] Yogesh Singh and S. Ramakrishnan, Phys. Rev. B **69**, 174423 (2004)
  - [13] J. A. Gotaas, J. W. Lynn, R. N. Shelton, P. Klavins, and H. F. Braun, Phys. Rev. B **36**, 7277 (1987)
  - [14] M. Nakashima, H. Kohara, A. Thamizhavel, T. D. Matsuda, Y. Haga, M. Hedo, Y. Uwatoko, R. Settai, and Y. Onuki, J. Phys.: Condens. Matter **17**, 4539 (2005)
  - [15] S. Noguchi and K. Okuda, Physica B **194-196**, 1975 (1994)
  - [16] Chandan Mazumdar, K. Ghosh, S. Ramakrishnan, R. Nagarajan, L. C. Gupta, G. Chandra, B. D. Padalia, and R. Vijayaraghavan, Phys. Rev. B **50**, 13879 (1994)
  - [17] C. B. Vining, R. N. Shelton, H. F. Braun, and M. Pelizzone, Phys. Rev. B **27**, 2800 (1983)
  - [18] Y. Nakajima, T. Nakagawa, T. Tamegai, and H. Harima, Phys. Rev. Lett. **100**, 157001 (2008)
  - [19] R. T. Gordon, M. D. Vannette, C. Martin, Y. Nakajima, T. Tamegai, and R. Prozorov, Phys. Rev. B **78**, 024514 (2008)

- [20] Y. Machida, S. Sakai, K. Izawa, H. Okuyama, and T. Watanabe, Phys. Rev. Lett. **106**, 107002 (2011)
- [21] Yasuyuki Nakajima, Hikaru Hidaka, Tsuyoshi Nakagawa, Tsuyoshi Tamegai, Terukazu Nishizaki, Takahiko Sasaki, and Norio Kobayashi, Phys. Rev. B **85**, 174524 (2012)
- [22] R. Gumeniuk, W. Schnelle, H. Rosner, M. Nicklas, A. Leithe-Jasper, and Yu. Grin, Phys. Rev. Lett. **100**, 017002 (2008)
- [23] Dong-Jin Jang, J. B. Hong, Y. S. Kwon, T. Park, K. Gofryk, F. Ronning, J. D. Thompson, and Yunkyu Bang, Phys. Rev. B **85**, 180505 (2012)
- [24] U. Stockert, M. Abdel-Hafiez, D. V. Evtushinsky, V. B. Zabolotnyy, A. U. B. Wolter, S. Wurmehl, I. Morozov, R. Klingeler, S. V. Borisenko, and B. Büchner, Phys. Rev. B **83**, 224512 (2011)
- [25] B. K. Cho, P. C. Canfield, L. L. Miller, D. C. Johnston, W. P. Beyermann, and A. Yatskar, Phys. Rev. B **52**, 3684 (1995)

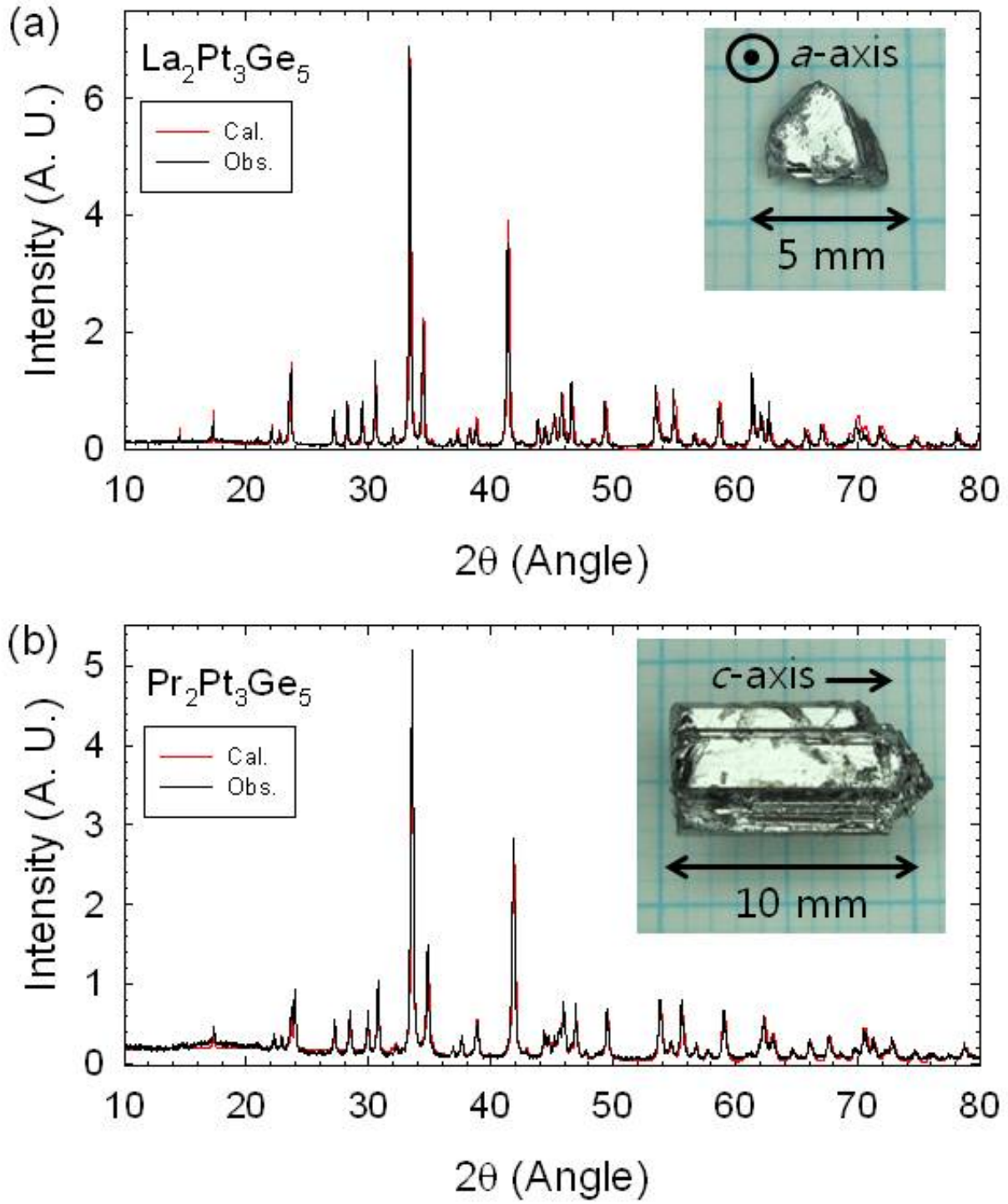


Fig. 1

FIG. 1: Powder XRD pattern of pulverized single crystals (black solid line) and refinement results (red solid line) of (a)  $\text{La}_2\text{Pt}_3\text{Ge}_5$  and (b)  $\text{Pr}_2\text{Pt}_3\text{Ge}_5$ . The insets in (a) and (b) show the morphology of single crystals of  $\text{La}_2\text{Pt}_3\text{Ge}_5$  and  $\text{Pr}_2\text{Pt}_3\text{Ge}_5$ , respectively.



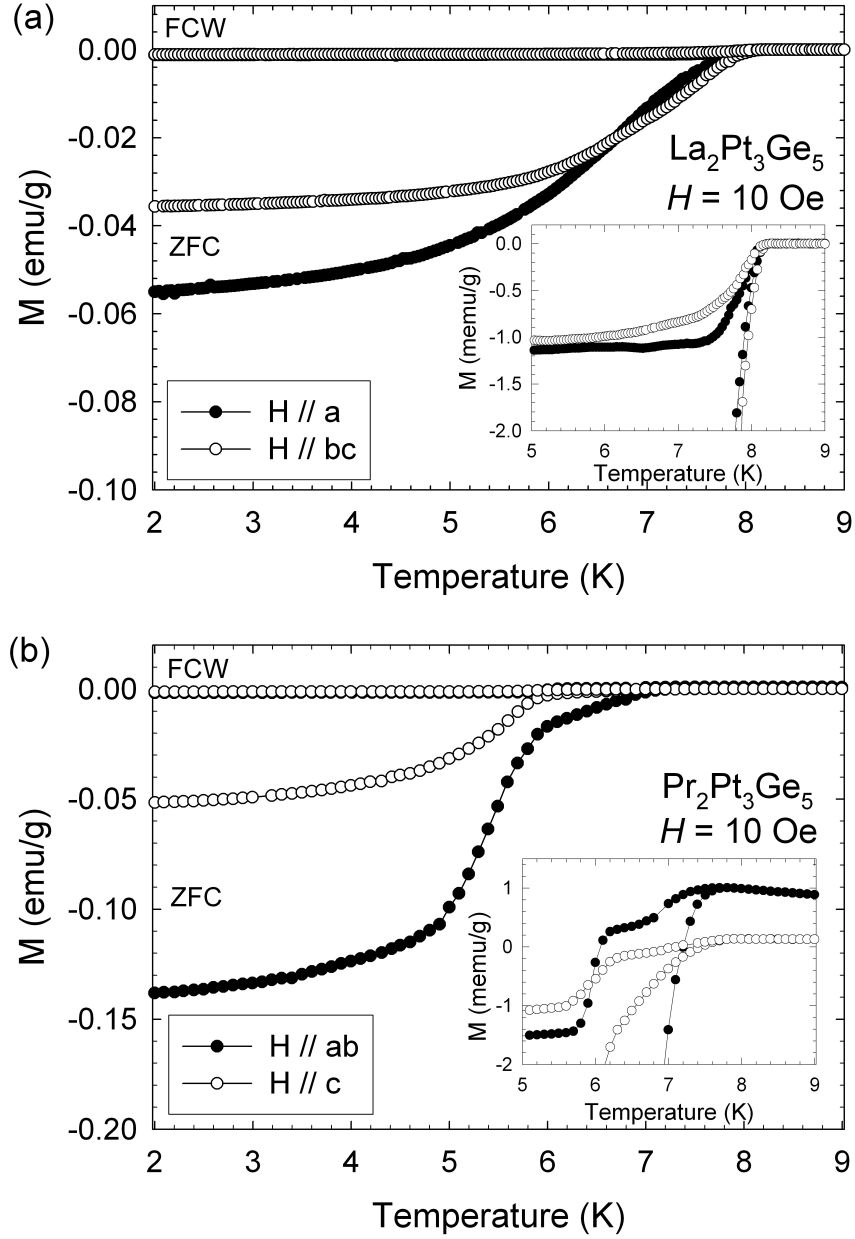


Fig. 2

FIG. 2: Temperature dependence of magnetization in zero-field-cooled (ZFC) and field-cooled-warming (FCW) modes: (a) for  $\text{La}_2\text{Pt}_3\text{Ge}_5$  single crystal with applied field of  $H = 10$  Oe being parallel ( $H \parallel a$ ) and perpendicular ( $H \parallel bc$ ) to the  $a$ -axis, and (b) for  $\text{Pr}_2\text{Pt}_3\text{Ge}_5$  single crystal with applied field of  $H = 10$  Oe being parallel ( $H \parallel c$ ) and perpendicular ( $H \parallel ab$ ) to the  $c$ -axis. Insets of (a) and (b): Expanded plots around  $T_c$  of  $\text{La}_2\text{Pt}_3\text{Ge}_5$  and  $\text{Pr}_2\text{Pt}_3\text{Ge}_5$ , respectively.

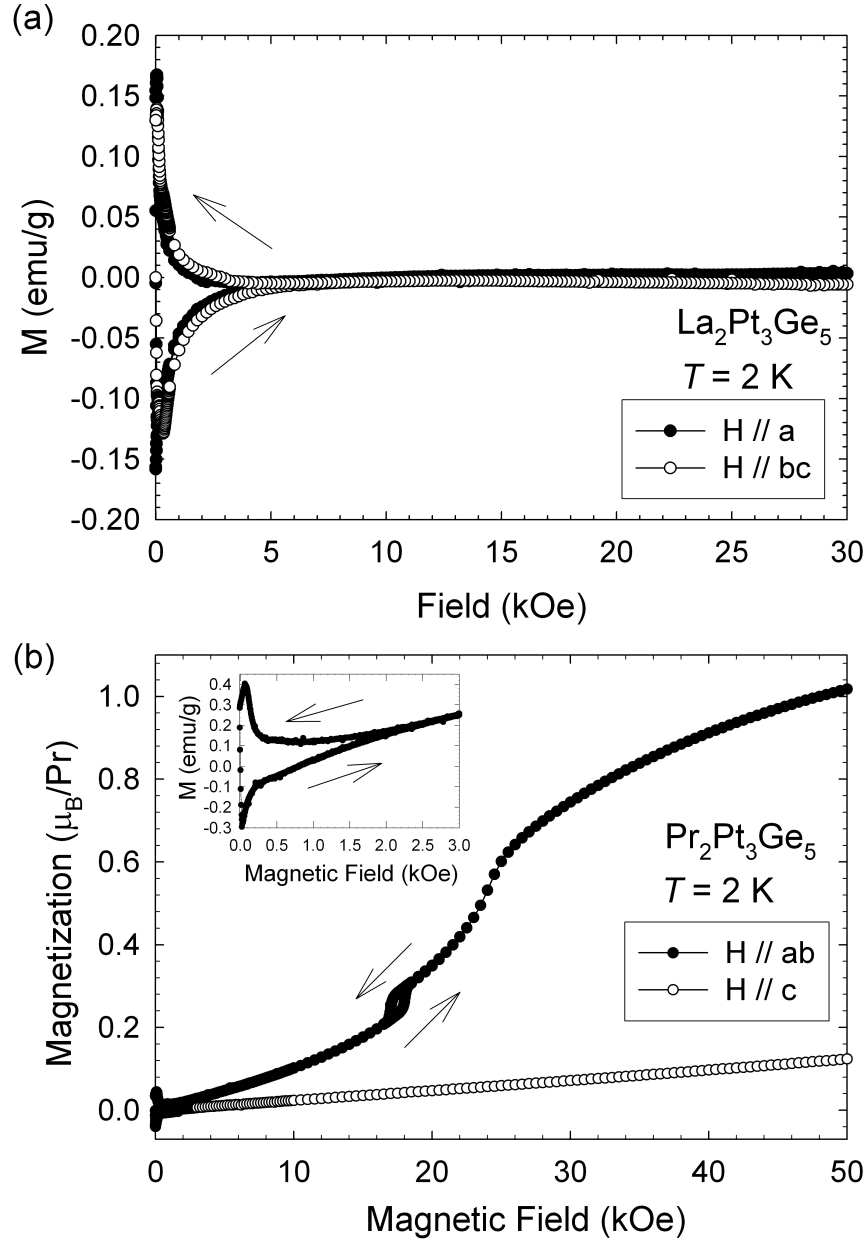


Fig. 3

FIG. 3: Isothermal magnetization at  $T = 2$  K: (a) for  $\text{La}_2\text{Pt}_3\text{Ge}_5$  single crystal with applied field being parallel ( $H \parallel a$ ) and perpendicular ( $H \parallel bc$ ) to the  $a$ -axis, and (b) a  $\text{Pr}_2\text{Pt}_3\text{Ge}_5$  single crystal with applied field being parallel ( $H \parallel c$ ) and perpendicular ( $H \parallel ab$ ) to the  $c$ -axis. Inset of (b): Expanded plot in a low field region ( $H \parallel ab$ ).

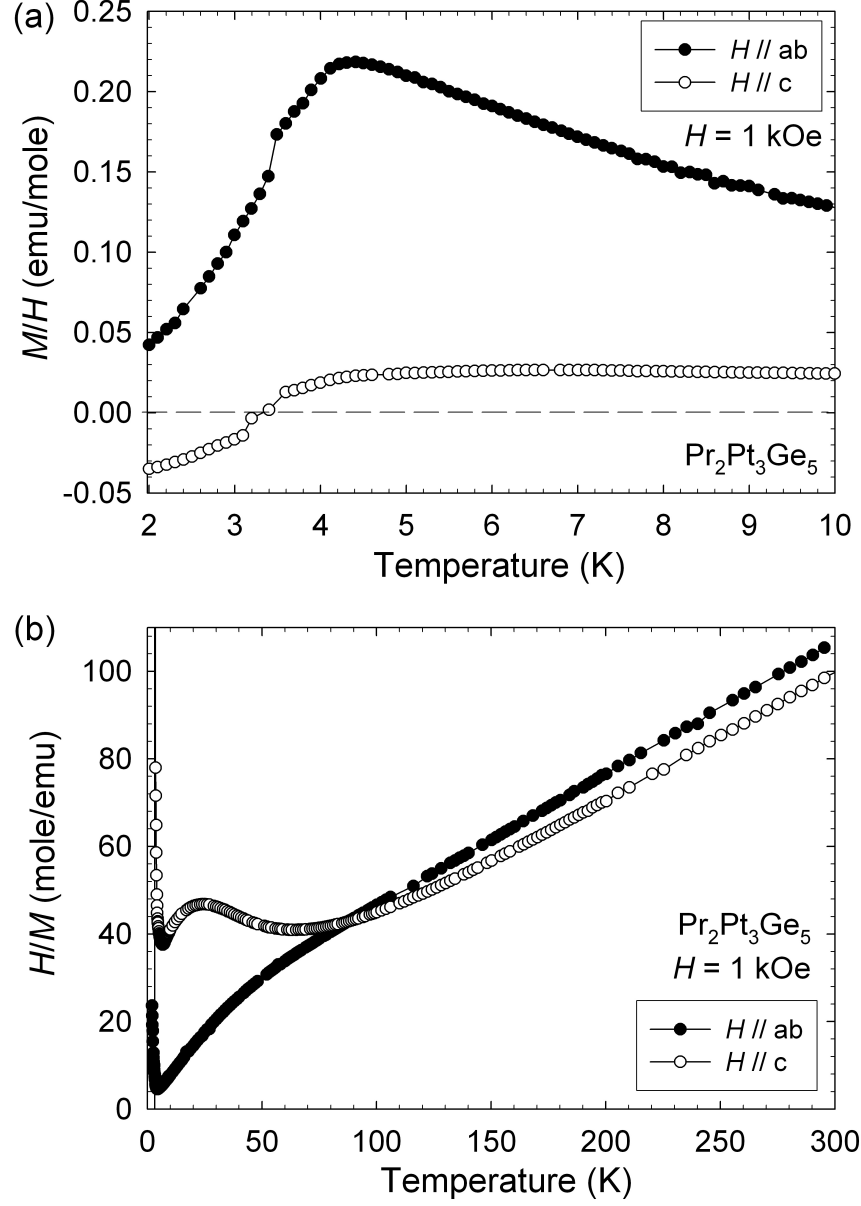


Fig. 4

FIG. 4: (a) Magnetization of  $\text{Pr}_2\text{Pt}_3\text{Ge}_5$  single crystal, divided by field of  $H = 1$  kOe,  $M/H$  in terms of temperature at low temperature region and (b) inverse magnetization of  $\text{Pr}_2\text{Pt}_3\text{Ge}_5$  single crystal, divided by field of  $H = 1$  kOe,  $H/M$  in terms of temperature in a temperature range  $2 \text{ K} \leq T \leq 300 \text{ K}$ : Close and open symbols for field perpendicular ( $H \parallel ab$ ) and parallel ( $H \parallel c$ ) to the  $c$ -axis, respectively.

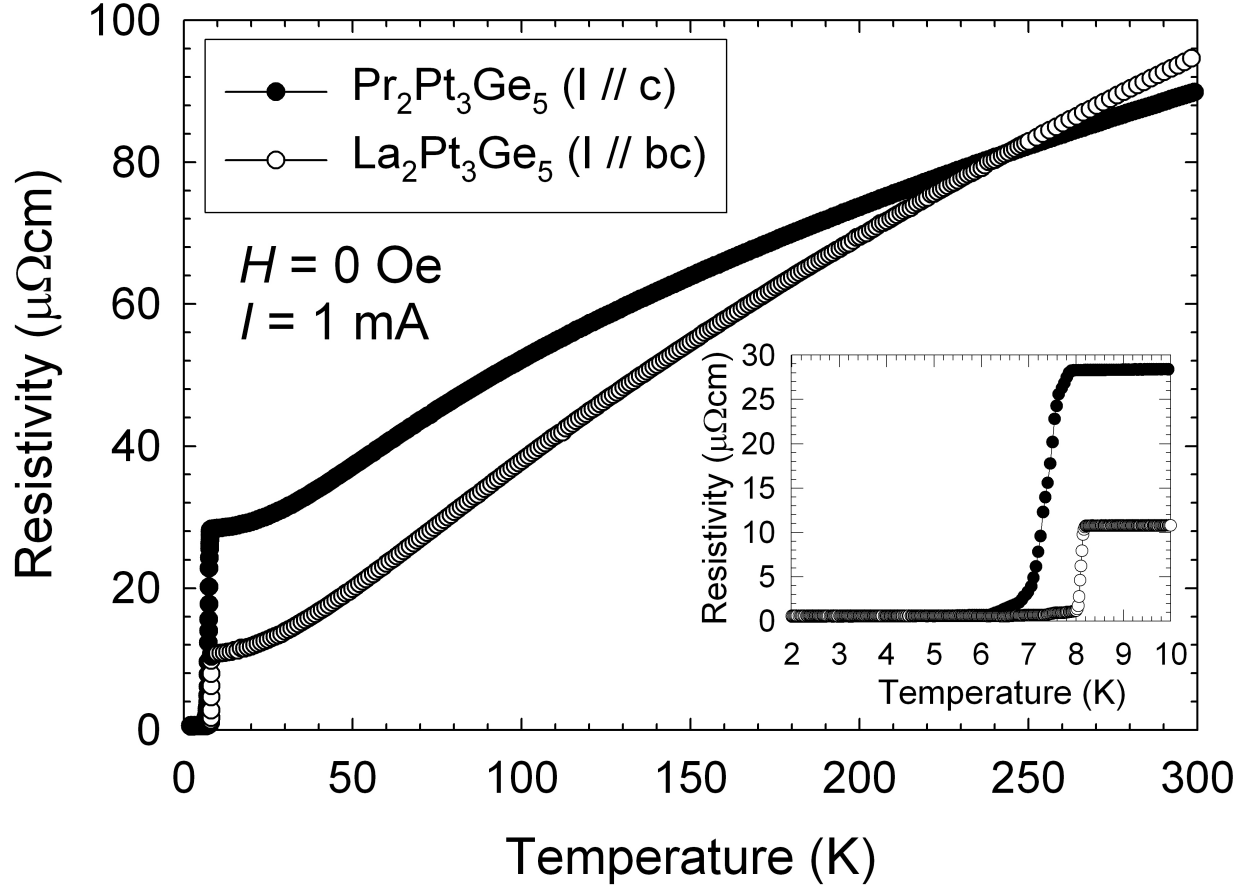


Fig. 5

FIG. 5: Temperature dependence of electrical resistivity up to  $T = 300$  K at  $H = 0$  Oe of  $\text{Pr}_2\text{Pt}_3\text{Ge}_5$  single crystal (close symbols) with a current parallel to the  $c$ -axis ( $I \parallel c$ ), and  $\text{La}_2\text{Pt}_3\text{Ge}_5$  single crystal (open symbols) with a current perpendicular to the  $a$ -axis ( $I \parallel bc$ ). Inset: Temperature-dependent resistivity in a low temperature region.

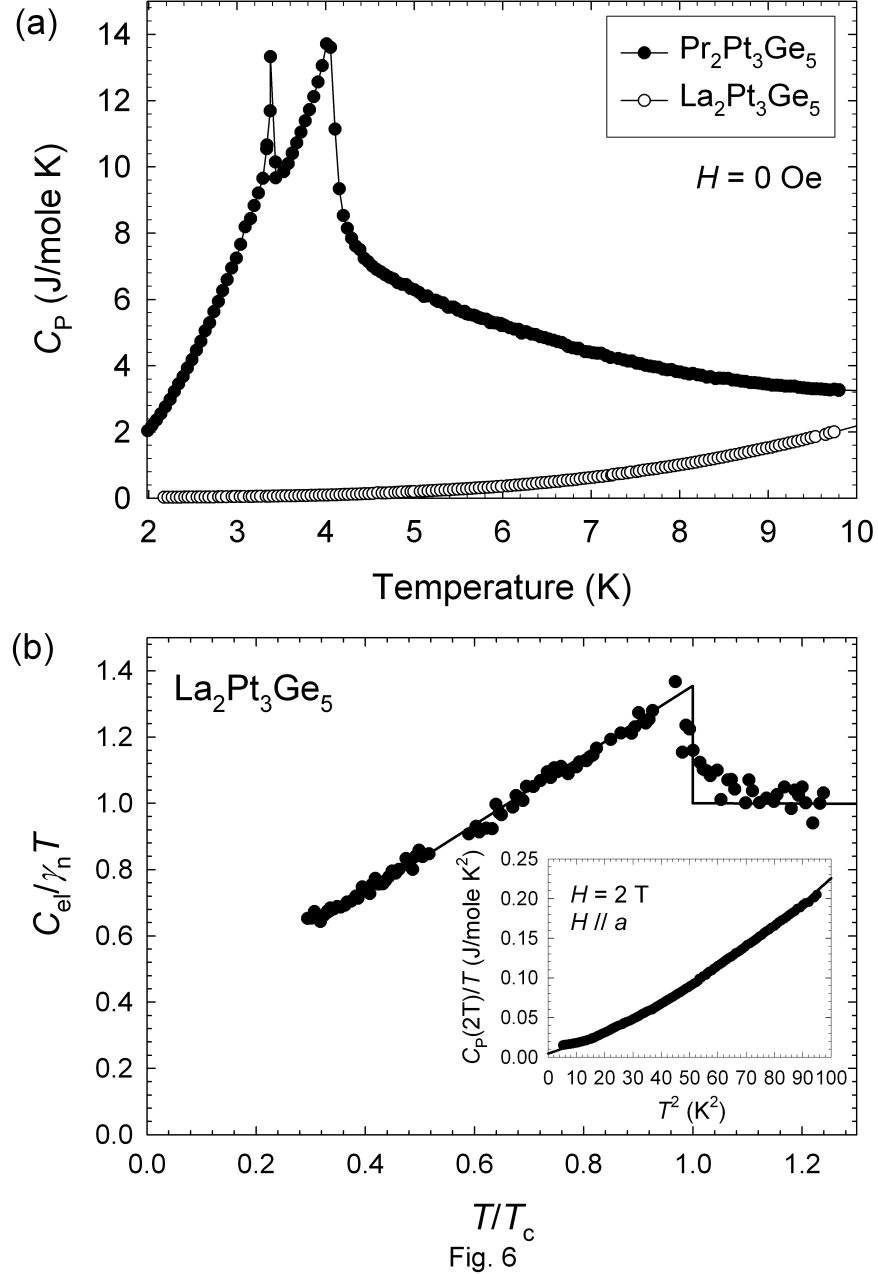


FIG. 6: (a) Specific heat of  $\text{Pr}_2\text{Pt}_3\text{Ge}_5$  single crystal (close symbols) and  $\text{La}_2\text{Pt}_3\text{Ge}_5$  single crystal (open symbols) at zero field in terms of temperature. (b) Normalized electronic specific heat coefficient of  $\text{La}_2\text{Pt}_3\text{Ge}_5$  single crystal. The solid lines is a guide to the eye. Inset of (b): Specific heat of  $\text{La}_2\text{Pt}_3\text{Ge}_5$  with applied field of  $H = 2$  T. The solid line is an estimated normal state specific heat from a polynomial form (see the text).